

---

This is an electronic reprint of the original article.  
This reprint may differ from the original in pagination and typographic detail.

Torkan, Masoud; Uotinen, Lauri; Nieminen, Ville; Rinne, Mikael

## Photogrammetry based characterization of hydro-mechanical properties of a rock fracture

*Published in:*

IOP Conference Series: Earth and Environmental Science

*DOI:*

[10.1088/1755-1315/833/1/012019](https://doi.org/10.1088/1755-1315/833/1/012019)

Published: 06/09/2021

*Document Version*

Publisher's PDF, also known as Version of record

*Published under the following license:*

CC BY

*Please cite the original version:*

Torkan, M., Uotinen, L., Nieminen, V., & Rinne, M. (2021). Photogrammetry based characterization of hydro-mechanical properties of a rock fracture. *IOP Conference Series: Earth and Environmental Science*, 833(1), Article 012019. <https://doi.org/10.1088/1755-1315/833/1/012019>

---

This material is protected by copyright and other intellectual property rights, and duplication or sale of all or part of any of the repository collections is not permitted, except that material may be duplicated by you for your research use or educational purposes in electronic or print form. You must obtain permission for any other use. Electronic or print copies may not be offered, whether for sale or otherwise to anyone who is not an authorised user.

PAPER • OPEN ACCESS

## Photogrammetry based characterization of hydro-mechanical properties of a rock fracture

To cite this article: M Torkan *et al* 2021 *IOP Conf. Ser.: Earth Environ. Sci.* **833** 012019

View the [article online](#) for updates and enhancements.



**ECS** **240th ECS Meeting**  
Digital Meeting, Oct 10-14, 2021  
**We are going fully digital!**  
Attendees register for free!  
**REGISTER NOW**

# Photogrammetry based characterization of hydro-mechanical properties of a rock fracture

M Torkan, L Uotinen, V Nieminen and M Rinne

Aalto University, Espoo, Finland

masoud.torkan@aalto.fi

**Abstract.** Hydro-mechanical properties of a single fracture are governed by several parameters such as contact area, roughness, tortuosity, aperture, channeling, matedness, sample sizes, normal stress, flow regime, and flow boundary conditions. In this study, photogrammetry with numerical modeling and laboratory measurements were used to investigate the influences of roughness, normal stress, aperture, water pressure, and different flow boundary conditions on fluid flow in an artificial granite fracture. A Finnish Kuru grey granite block was mechanically split, and a 250 mm × 250 mm × 100 mm slab pair sample with a tensile crack in the middle was extracted. A photogrammetry-based method was used to reconstruct a 3D model of the fracture geometry. The resulting model was numerically simulated with COMSOL using the Navier-Stokes equations. Fluid flow experiments were computed with the Forchheimer equation. Comparison between the numerical modeling results and the analytical solution confirms that the 3D roughness geometry has a crucial role in defining the transmissivity, especially for nonlinear flow. On the other hand, normal stress increases fracture closure and increases contact areas, decreasing the hydraulic aperture and changing the flow paths. The presented method can be used in the contactless estimation of fluid flow properties of rock joints.

## 1. Introduction

The flow of ground water in fractured bedrock is an essential problem when considering the usage of rock mass as a barrier to prevent radionuclides escaping from a geological spent nuclear fuel repository. Fracture geometry, joint roughness, and joint aperture are key parameters affecting the flow properties in rock joints. The knowledge of the fluid flow phenomena in the bedrock forms the basis of evaluating the transportation of the fluid in the bedrock. The bedrock in depth is under significant loading due to the weight of the overlying rock and tectonic movements. The stress state of the bedrock will change during time, and the excavations and filling of the tunnels will cause changes in the stress state of the bedrock. These are aspects that should be considered with applications such as tunnel construction, deep underground repository system, or groundwater management.

The flow path of groundwater varies when the stress field in bedrock undergoes changes and on the other hand, groundwater alters the effective stress state in rock fractures. Fluid affects the stress state in the rock and thus can create new flow paths and the stress state affects to the opening and closing of the flow paths as well the fracture aperture. In this sense, the situation can be regarded as a connected hydro-mechanical problem. In terms of nuclear waste management, hydro-mechanical modelling is part of thermo-hydro-mechanic-chemical (THMC) modelling. Connected hydro-mechanical problem has a two-way connection, so it can be viewed separately from temperature and chemical processes when not operating in the immediate vicinity of the repository tunnels. The hydro-mechanical processes of a single



rock joint are dependent on the properties of that single rock joint as well as the properties of the rock joints that are connected to it, and their geometry, orientation and the effective stress of the fracture walls [1].

Fluid flow in a single fracture in fractured rock masses is studied extensively by several authors [1-6]. Also, a number of experimental studies have been carried out where the effects of three-dimensional stress field on a fluid flow through rock fracture are studied [7-18]. Flow properties of small-scale rock fractures are well-studied, which creates the need to move towards a larger scale to validate the results acquired from small-scale laboratory studies.

## 2. Methodology

### 2.1. Photogrammetry procedure

The photogrammetry procedure is a three-phase method. In the first phase, both slabs are in tight contact, and each sample was fitted with circular targets for photogrammetry (figure 1a). Then target-to-target distances were manually measured with a digital caliper with the resolution of 0.1 mm, resulting in an accuracy of +/- 0.2 mm.

The sample is a pair set of 250 mm × 250 mm × 100 mm slabs with an artificially induced tensile fracture between them. The material is Kuru grey granite which is fairly homogenous and isotropic. Each sample half was photographed using a revolving table by taking 40 photographs per revolution (figures 1b and 1c). This process was conducted for two dip angles of the camera (30° and 60°). Then, the sample half was flipped upside down, and the process was repeated. To improve the accuracy of the method, a 4×4 grid consisting of square cells each with 5 cm side length, was used. At each grid node a photo was taken, 25 images for each surface. This results in a full exterior 3D reconstruction of the sample pair. This model was oriented and scaled using the measured distances between the circular targets. Each set of photographs is processed into a 3D model using the Reality Capture software (figure 1d). This results in three 3D models, one for the bottom and one for the top.

After this stage, the data of both halves were placed in the same coordinate system according to the circular targets. Finally, the physical aperture distribution was calculated with the coordinated data of the top and bottom halves with CloudCompare software (figure 1e and 1f). The photos were captured by using Canon 5DS R DSLR camera and Canon 35 mm f/1.4L II USM objective.

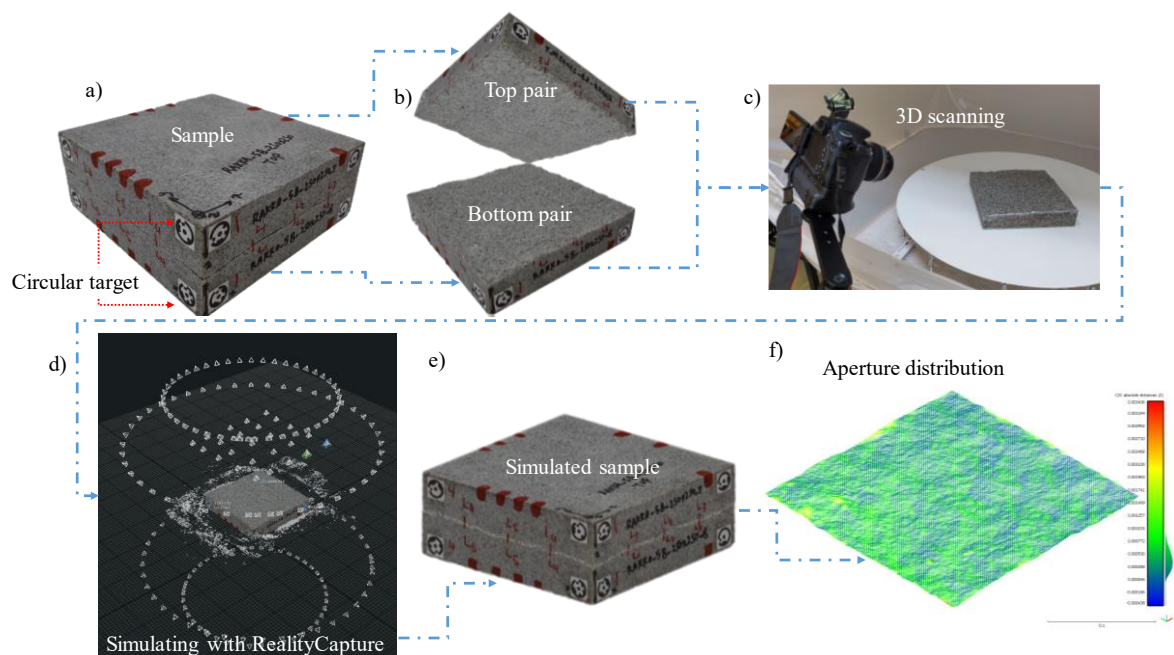


**Figure 1.** Photogrammetry and measurement procedures of fracture morphologies.

2.2. Water flow test

Water flow tests were performed by using a laboratory circuit shown in figure 2. The circuit consists of a hydraulic jack unit to apply normal pressures on samples, a data logger to record data. A water tank, compressed air and an adjustable air regulator apply constant water pressures to one side of the fracture. A pressure transducer was attached to the water inlet to measure the inlet water pressure. A plate was used to equalize normal pressures on samples' top surfaces. The normal stress was 0.5 MPa. The discharge water was measured by a digital balance with a precision of 0.01 g. Ten water pressures were chosen to conduct these tests, ranging from 5 kPa to 50 kPa with 5 kPa intervals. The experimental tests were conducted in the civil engineering laboratory at Aalto University. The temperature is 25° C, and the density and dynamic viscosity of water are  $\rho = 0.997 \times 10^3 \text{kg/m}^3$  and  $\mu = 0.89 \times 10^{-3} \text{Pa.s}$ , respectively. To seal the lateral sides of the sample, a self-designed frame was used (figure 3). This frame can control pathways of inlets and outlets in preferred directions. The internal faces of the frame were covered by the rubber to avoid leakage of the sample. The inlets and outlets were controlled by valves to be selected water flow directions. Silicon glue and tape were used to seal the corner of the sample to prevent the connection between sides. To detect amounts of vertical movements of the fracture after applying normal stress, four LVDTs were installed around the sample (figure 4).

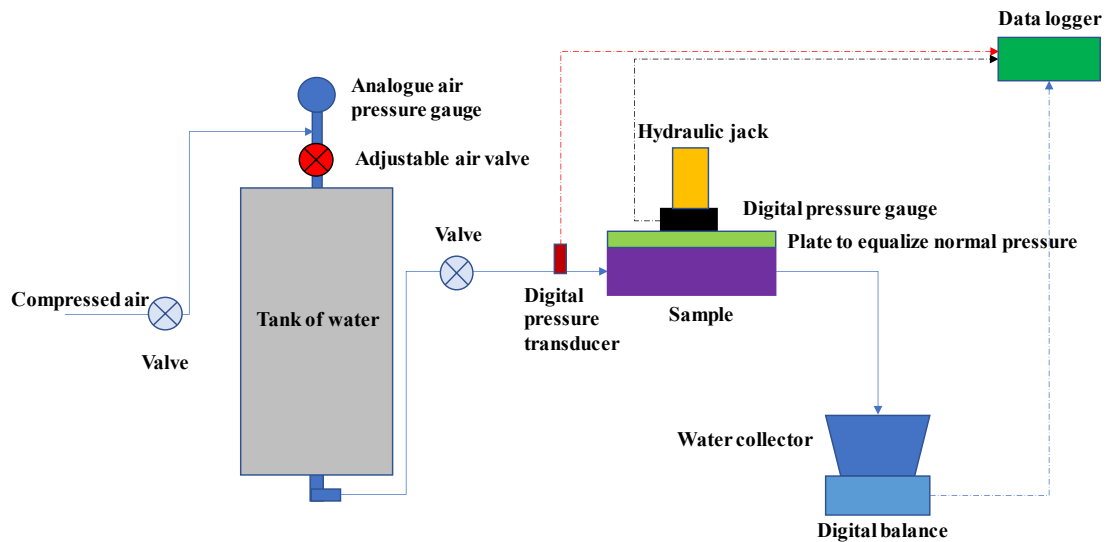


Figure 2. Schematic of the hydraulic test.

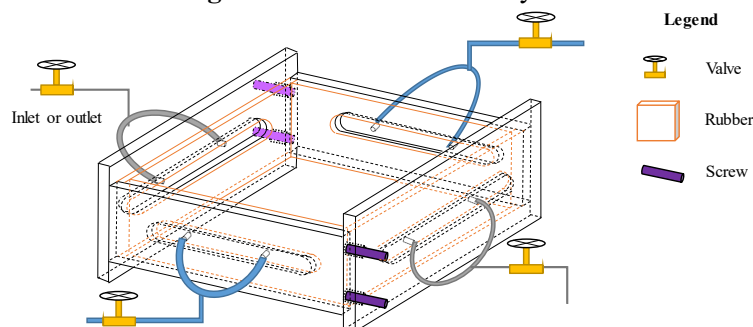
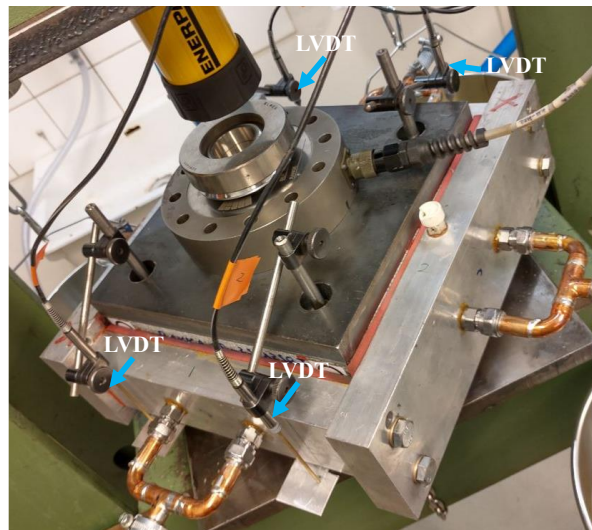


Figure 3. Diagram of the self-designed frame to test the water flow.



**Figure 4.** Locations of LVDTs.

### 2.3. Background theory

The Forchheimer equation [19] is adopted to characterize the flow through a rough fracture (1),(2),(3).

$$-\nabla P = aQ + bQ^2 \quad (1)$$

$$a = \frac{12\mu}{we_h^3} \quad (2)$$

$$b = \frac{\beta\rho}{w^2e_h^2} \quad (3)$$

where  $\nabla P$  is the hydraulic gradient (Pa/m),  $a$  ( $\text{kg/m}^5\text{s}$ ) and  $b$  ( $\text{kg/m}^8$ ) denote viscous and inertial effects, respectively,  $Q$  is flowrate ( $\text{m}^3/\text{s}$ ),  $w$  indicates the width of the fracture (m),  $e_h$  signifies the hydraulic fracture (m),  $\mu$  is the dynamic viscosity of water ( $\text{Pa}\cdot\text{s}$ ),  $L$  represents the length of the fracture (m) and  $\beta$  characterises nonlinear coefficient, and  $\rho$  represents the fluid density ( $\text{kg/m}^3$ ).

The numerical modelling was solved by the Navier-Stokes equations (NSE) for water as incompressible and single Newtonian fluid flow in the COMSOL software. The NSE is written as equations (4) and (5) [20],[21]:

$$\rho(\mathbf{u}\cdot\nabla)\mathbf{u} + \nabla P = \mu\nabla^2\mathbf{u} \quad (4)$$

$$(\nabla\cdot\mathbf{u})=0 \quad (5)$$

where  $\mathbf{u}$  is the flow velocity vector. In equation (4), the term  $\mu\nabla^2\mathbf{u}$  represents the viscous force, and the convective acceleration terms  $\mathbf{u}\cdot\nabla\mathbf{u}$ , representing the inertial forces acting on the fluid, giving rise to the nonlinearity of the equation and increase the computational cost.

### 2.4. Numerical modelling setup

The point clouds of rough surfaces obtained by the photogrammetry were regenerated with parametric surface function in the COMSOL software. Contact areas were identified and removed. Due to the scale of the sample, the numerical model was portioned to small parts. The parts were then meshed with normal size. To regenerate the fracture under normal stress, the averaged value of the vertical movements obtained from the LVDTs, was decreased from the height values of the top surface. After that, the fracture was reconstructed by using the aforementioned method. Suitable initial and boundary conditions were assigned for the flow simulation (figure 5). The top and bottom surfaces and the side

boundaries of the fracture were defined as impermeable and non-slip boundaries. The constant water pressure was applied along the inlet and the zero pressure alongside the outlet.

### 3. Result and Discussion

#### 3.1. Experimental results

The mean of the vertical distances between two fracture surfaces, obtained from the photogrammetry, was 0.462 mm (figure 6). The average of the vertical movements, measured by the LVDTs after applying normal stress, was 0.077 mm. The physical aperture under normal stress was 0.385 mm. By enhancing normal stress, the contact areas increase. figures 5a and 5b show the same morphologies of a fracture but under two normal stress conditions, 0 MPa and 0.5 MPa. As it can be seen, in figure 5b (0.5 MPa) there are more contact areas than in figure 5a (0 MPa).

Figure 7 illustrates the results of 20 water flow tests through the fracture. In each condition, 10 tests with different water pressures were done. The relationship between the pressure gradient ( $\nabla P$ ) and flow rate ( $Q$ ) is polynomial. It means the fluid behaviour is nonlinear and the data fits the Forchheimer equation better. By using best-fit regression the coefficients in the Forchheimer equation were gained (table 1). The hydraulic aperture was reduced by increasing the normal stress because of increasing contact areas.

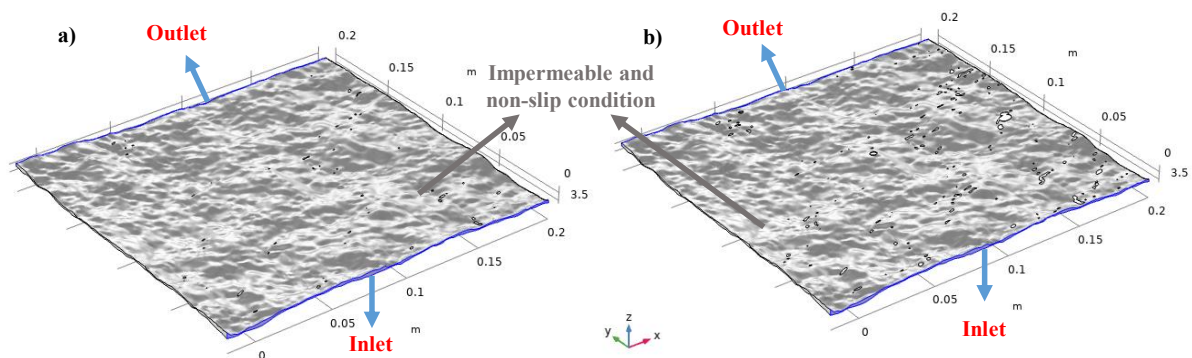


**Figure 5.** Boundary conditions for flow simulation for the fracture without normal stress (a) and the fracture under 0.5 MPa normal stress (b).

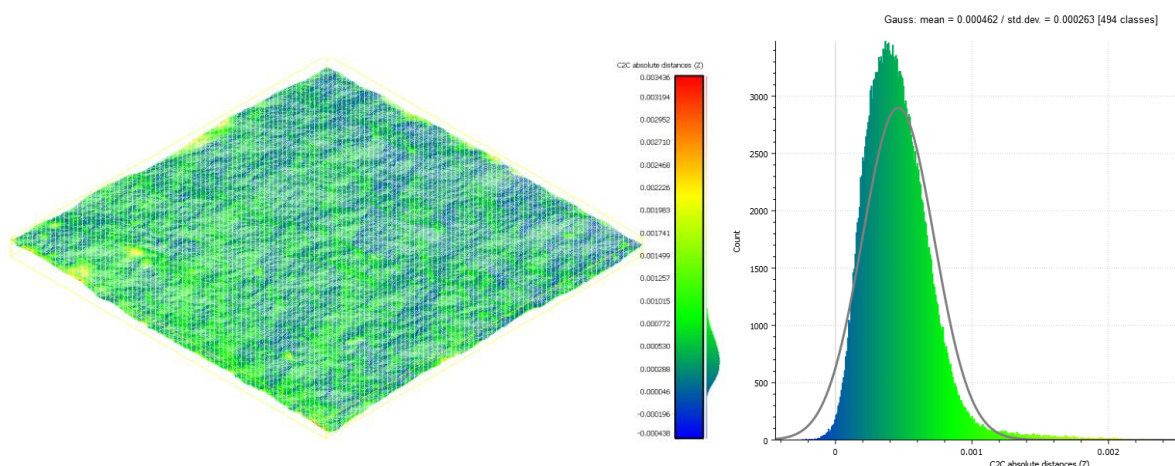


**Figure 6.** The distribution of the physical aperture of the fracture.

**Table 1.** Parameters obtained from the Forchheimer equation for flow in fractured samples.

Condition	Parameters		
	a (kg/m <sup>5</sup> s)	b (kg/m <sup>8</sup> )	e <sub>h</sub> (mm)
Without normal stress	3.79×10 <sup>9</sup>	5.48×10 <sup>13</sup>	0.2242
Under normal stress	1.6×10 <sup>10</sup>	4.39×10 <sup>14</sup>	0.1387

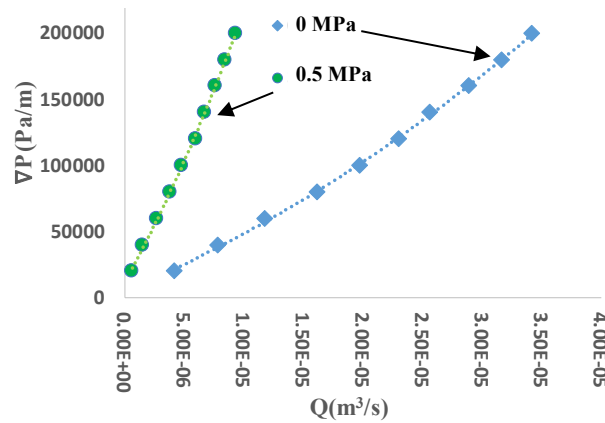
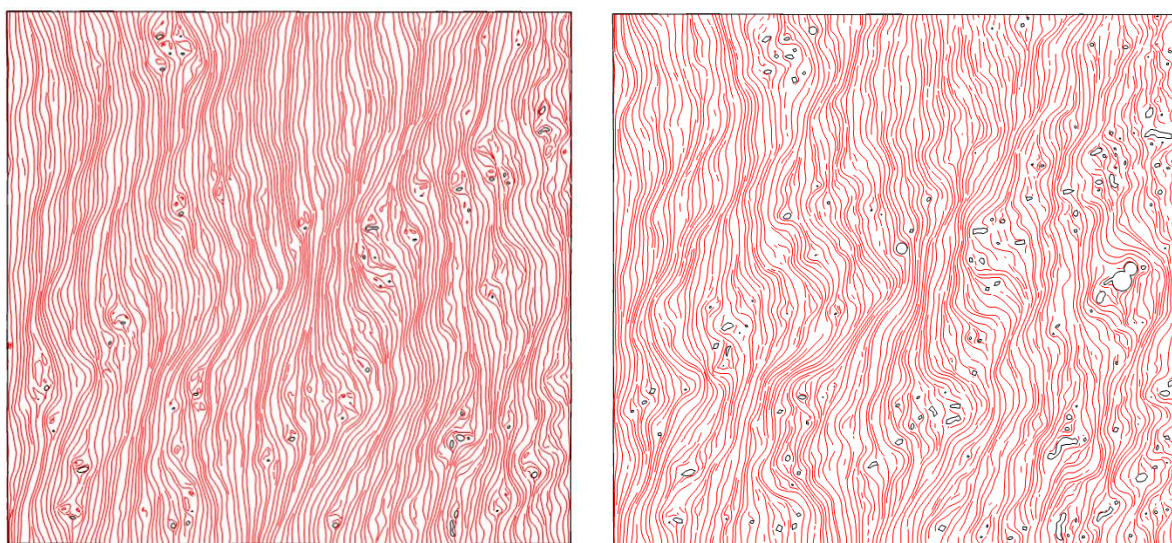


**Figure 7.** Regression analysis of measured pressure gradient as a function of flow rate using the Forchheimer equation for the fracture without normal stress (0 MPa) and under normal stress (0.5 MPa).

3.2. Numerical results

The simulated streamlines under two normal stress conditions are depicted in figure 8. As can be seen, the streamline distribution in figure 8a is more channelized and uniformly than figure 8b. After applying normal stress, the contact areas and void spaces increased, resulting in tortuosity behaviour of the flow through the fracture. The comparison of figures 8a and 8b show the uniformity of the streamline distribution was affected by increased normal pressure. It means the streamlines at 0 MPa normal stress exhibit more linearity than 0.5 MPa. Normal stress decreases the physical aperture, and in some regions, the fluid flow was blocked due to the new contact areas or small local apertures. Around the contact areas, the streamlines are more nonlinear. This illustrated that the fluid flow has nonlinear behaviour through a rough fracture.



(a) Normal stress 0 MPa

(b) Normal stress 0.5 MPa

**Figure 8.** The simulated streamlines of flow through the scanned fracture under two normal stresses of 0 MPa (a) and 0.5 MPa (b) with the same water pressure of 50 kPa.

#### 4. Conclusion

In this study, 20 flow tests were performed on 250 mm × 250 mm artificial tensile crack with two normal stress conditions of 0 MPa and 0.5 MPa. The experimental results show the relationship between water pressure gradient and the flow rate is not linear and can be better described by the Forchheimer equation. The coefficients of this equation were measured by increasing the normal stress. Based on the results, it appears that these coefficients are related to the physical aperture. Photogrammetry can be used to obtain the physical aperture with high precision.

The regime of flow changed when the contact areas increased under normal stress. The streamlines for the larger physical aperture were channelized. It means that flow can move straightforwardly through the fracture. However, by increasing the normal stress, tortuosity was observed around the contact areas. It seems that the water pressure would drop because of the resistance of contact areas through the fracture. This leads to an increased possibility nonlinear flow.

#### Acknowledgements

The authors gratefully thank the Finnish Nuclear Waste Management fund VYR and the KYT2022 research programme for funding.

#### References

- [1] Zimmerman, R. & Main, I. 2004. Hydro-mechanical behaviour of fractured rocks. International Geophysics Series, 89, pp. 363-422.
- [2] Brown, S., Caprihan, A. & Hardy, R. 1998. Experimental observation of fluid flow channels in a single fracture. *Journal of Geophysical Research: Solid Earth*, 103(B3), 5125-5132.
- [3] Isakov, E., Ogilvie, S. R., Taylor, C. W. & Glover, P. W. 2001. Fluid flow through rough fractures in rocks I: high resolution aperture determinations. *Earth and Planetary Science Letters*, 191(3-4), 267-282.
- [4] Ogilvie, S. R., Isakov, E. & Glover, P. W. 2006. Fluid flow through rough fractures in rocks. II: A new matching model for rough rock fractures. *Earth and Planetary Science Letters*, 241(3-4), 454-465.
- [5] Yasuhara, H., Polak, A., Mitani, Y., Grader, A. S., Halleck, P. M. & Elsworth, D. 2006. Evolution of fracture permeability through fluid-rock reaction under hydrothermal conditions. *Earth and Planetary Science Letters*, 244(1-2), 186-200.
- [6] Ferer, M., Crandall, D., Ahmadi, G. & Smith, D. H. 2011. Two-phase flow in a rough fracture: Experiment and modeling. *Physical Review E*, 84(1), 016316.
- [7] Barton, N.R. & Choubey, V. 1977. The shear strength of rock joints in theory and practice. *Rock Mechanics*. Vol. 10:1-2. S. 1-54.
- [8] Bandis, S., Lumsden, A. C. & Barton, N. R. 1981. Experimental studies of scale effects on the shear behaviour of rock joints. In *International journal of rock mechanics and mining sciences & geomechanics abstracts* (Vol. 18, No. 1, pp. 1-21). Pergamon.
- [9] Yeo, I. W., De Freitas, M. H. & Zimmerman, R. W. 1998. Effect of shear displacement on the aperture and permeability of a rock fracture. *Int. J. Rock Mech. Min. Sci.*, 35(8), 1051-1070.
- [10] Lee, H. S. & Cho, T. F. 2002. Hydraulic characteristics of rough fractures in linear flow under normal and shear load. *Rock Mechanics and Rock Engineering*, 35(4), 299-318.
- [11] Min, K. B., Rutqvist, J., Tsang, C. F. & Jing, L. 2004. Stress-dependent permeability of fractured rock masses: a numerical study. *International Journal of Rock Mechanics and Mining Sciences*, 41(7), 1191-1210.
- [12] Jiang, Y., Xiao, J., Tanabashi, Y. & Mizokami, T. 2004. Development of an automated servo-controlled direct shear apparatus applying a constant normal stiffness condition. *Int. J. Rock Mech. Min. Sci.*, 41(2), 275-286.
- [13] Saito, R., Ohnishi, Y., Nishiyama, S., Yano, T. & Uehara, S. 2005. Hydraulic characteristics of single rough fracture under shear deformation. In *ISRM International Symposium-EUROCK 2005*. ISRM.

- [14] Li, B., Jiang, Y., Koyama, T., Jing, L. & Tanabashi, Y. 2008. Experimental study of the hydro-mechanical behavior of rock joints using a parallel-plate model containing contact areas and artificial fractures. *International Journal of Rock Mechanics and Mining Sciences*, 45(3), 362-375.
- [15] Nemoto, K., Watanabe, N., Hirano, N. & Tsuchiya, N. 2009. Direct measurement of contact area and stress dependence of anisotropic flow through rock fracture with heterogeneous aperture distribution. *Earth and Planetary Science Letters*, 281(1-2), 81-87.
- [16] Nemoto, K., Watanabe, N., Hirano, N. & Tsuchiya, N. 2009. Direct measurement of contact area and stress dependence of anisotropic flow through rock fracture with heterogeneous aperture distribution. *Earth and Planetary Science Letters*, 281(1-2), 81-87.
- [17] Rong, G., Yang, J., Cheng, L. & Zhou, C. 2016. Laboratory investigation of nonlinear flow characteristics in rough fractures during shear process. *Journal of hydrology*, 541, 1385-1394.
- [18] Wang, C., Jiang, Y., Luan, H., Liu, J. & Sugimoto, S. 2019. Experimental Study on the Shear-Flow Coupled Behavior of Tension Fractures Under Constant Normal Stiffness Boundary Conditions. *Processes*, 7(2), 57.
- [19] Qian, X., Xia, C., Gui, Y., Zhuang, X., & Yu, Q. 2019. Study on flow regimes and seepage models through open rough-walled rock joints under high hydraulic gradient. *Hydrogeology Journal*, 27(4), 1329-1343.
- [20] Bear, J. 1972. *Dynamics of fluids in porous media*. Courier Corporation.
- [21] Zimmerman, R. W., & Bodvarsson, G.S. 1996. Hydraulic conductivity of rock fractures. *Transport in porous media*, 23(1), 1-30.